Active and Reactive Power Control based on Predictive Voltage Control in a Six-Phase Generation System using Modular Matrix Converters

S. Toledo, M. Ayala, E Maqueda, R. Gregor
Lab. of Power and Control Systems
Universidad Nacional de Asunción
Luque, Paraguay
{stoledo, mayala, emaqueda, rgregor}@ing.una.py

M. Rivera
Lab. of Energy Conversion and Power Electronics
Universidad de Talca
Curicó, Chile
marcoriv@utalca.cl

T. Dragicevic
Dept. of Energy Technology
Aalborg University
Aalborg, Denmark
tdr@et.aau.dk

P. Wheeler
Dept. of Electrical and Electronic Engineering
University of Nottingham
Nottingham, UK
pat.wheeler@nottingham.ac.uk

***Abstract*—Renewable energy generation systems under distributed generation frame emerges as a plausible solution for nowadays growing world energy demands. In this context multiphase wind generation systems are a feasible option that consist of renewable AC source that need efficient and totally controlled power conversion stages. In this work a novel active and reactive power control strategy based on two cascade control loops using a combination of classical PR controller and Model Based Predictive Voltage Control is proposed. Furthermore, the generator is a Permanent Magnet Synchronous Generator and the power stage is based on a multi-modular direct matrix converter topology providing interesting features to the scheme. The performance of the whole system is analysed regarding tracking of reference and THD with satisfying transient results and THD lower than 1.52 % in the injected current widely accomplishing with international standards.**

***Index Terms*—Distributed Generation System, Multi-modular Matrix Converter, Multi-phase Machines, Predictive Control, Predictive Voltage Control.**

I. INTRODUCTION

The new energy paradigm known as Distributed Generation Systems (DGS) is focused on the interaction between several energy sources, mainly using renewable energies (RES), interacting in a synergistic manner based on small-scale, decentralised, local on-side generation [1]. Wind energy harvesting emerges as one of the most promising sources under DGS scheme [2]–[4] and a very active research area is focused in multiphase wind energy generator (MWEG) systems [5]. Multiple three-phase windings in MWEG are very convenient for wind turbines (WT) and several studies employing these topologies have been conducted recently [6]. The possibility to split the power and the current between a higher numbers of phases, allowing the per-phase inverter power rating reduction is the main reason of selecting multiphase topologies for WT [5], [7], [8]. Moreover, this configuration guarantees WT working continuity, even in presence of phase and/or inverter faults. Hence, the use of multiphase electrical drives in WT should enable an increase of availability, the working time, and consequently, the annual energy yield, determining a reduction in the maintenance cost. In MWEG, the six-phase wind energy generator (SpWEG) with two sets of three-phase stator windings spatially shifted by 30 and 60 electrical degrees and isolated neutral points is probably one of the most widely discussed topology with fully rated back-to-back converter system to interconnect the energy source to the electrical network (grid), focused on distributed generation (DG) [9]–[11]. Furthermore, on DG systems the most widely used power electronic grid-connected converter (GCC) are the active front-end (AFE) [12], [13], cascaded multilevel converters [14], [15] and neutral-point-clamped (NPC) topologies [16], [17]. GCC topologies must ensure an efficient active and reactive flux control with minimum current and voltage harmonic distortions besides ensuring proper synchronisation with the grid. Several control methods have been addressed to accomplish this, such as: pulse width modulation (PWM), space vector modulation (SVM), fuzzy control, model based predictive control (MPC), etc. [18]–[21]. However, most converters used to interconnect the energy sources to the grid used storage energy elements (i.e. capacitor banks) which provide weight, volume and failure possibilities to the GCC topologies. Latest research efforts have been focused in the development of a flexible power interface

based on a modular architecture capable of interconnecting different RES under the DGS frame. In the past two proposal combining multi-phase machines and multi-modular direct matrix converters (MMC) have been proposed for induction machines, showing good performance in about mentioned applications [22], [23]. The main feature of this topologies consist of the ability to provide a three-phase sinusoidal voltages with variable amplitude and frequency using fully controlled bi-directional switches without the use of storage energies elements. These characteristics make plausible the use of MMC in applications where a high power density and compact converters are required, such as SpWEG systems, constituting an attractive alternative compared to conventional converter topologies [24]. The main contribution of this paper is the proposal of a novel power conversion control scheme for a SpWEG with a PMSG. The proposed control scheme is based on two control loops, one using a classical PR controller and anther based on Predictive Voltage Control applied to a multi-modular direct matrix converters in the power stage.

II. SIX-PHASE PERMANENT MAGNET SYNCHRONOUS GENERATOR

The six-phase PMSG operates at an identical value of average speed of the magnetic field established by the phase coils driving alternating currents. The equivalent circuit of the PMSG is similar to a DC machine, however, the electromagnetic analysis is more similar to induction machines, with the difference that rotor does not present connected bars, but permanent magnets which establish a fixed magnetic field that interacts with the rotating magnetic field generated by the alternating currents in the stator. On the other hand, from the point of view of physical construction, PMSG classify on salient poles and cylindrical rotor (uniform reluctance), the latter closely resembles to the induction machines from the electromagnetic point of view, since it has an uniform reluctance in its air gap, which greatly simplifies the mathematical analysis. It is also the most used type as a generator.

A. Generated Voltages and Equivalent Circuit

Based on circuit theory, an accurate behaviour analysis can be performed dynamic of the permanent magnet generator with the following equations:

$$B_{sa} = B_{mm} sin[p(\phi_s - \omega_s t)] \tag{1}$$

$$\phi_{fm} = \int B_{sa} dA \tag{2}$$

$$\phi_{fm} = \int_{-\frac{\pi}{2p}}^{\frac{\pi}{2p}} B_{mm} sin[p(\phi_s - \omega_s t)](\frac{D}{2} l d\phi_s) \tag{3}$$

$$\omega_s = \frac{\omega}{p} \tag{4}$$

$$\phi_{fm} = -\frac{2D}{2p} l B_{mm} sin[\omega t] \tag{5}$$

$$\phi_{fm} = -\Phi_m sin[\omega t] \tag{6}$$

where ϕ_s is the stator mechanical angle (winding), ω_s is the mechanical synchronous speed, ϕ_{fm} is the mutual flow of the rotor field, D is the inside diameter of the stator, l is the depth of the set of stator laminations, p is the pole pairs of the machine and ω is the electrical speed. The induced voltage in the windings can be obtained by applying Faraday laws and Lenz:

$$e_a = -N_{eff} \frac{d\phi_{fm}}{dt} = N_{eff} \omega \Phi_m cos[\omega t] \tag{7}$$

where N_{eff} is the winding by phase. The effective value of the voltage is determined on the basis of the phase sizing as follows:

$$\overline{E}_a = 4.44 N_{eff} f \Phi_m \tag{8}$$

where $\overline{E}_a$ is the effective value of the phase voltage a y f is the electric frequency of the stator currents.

At the same time, the balanced synchronous generator has an identical number of windings per phase (N_{eff}) at the stator and identical leakage inductance values (L_{sf}), self inductance (L_{ss}) and mutual inductance (M_s). Any inductance or reactance only needs to be determined by one of the windings per phase. It is assumed that the ferromagnetic structure is infinitely permeable and allows the direct addition of the flows, which has the following equation:

$$L_{ss} = \frac{N_{eff}(\phi_{sf} + \phi_{aM})}{i_a} = L_{sf} + L_{sM} \tag{9}$$

if $i_b = i_c = 0$, where i_a is the phase current a. To determine M_s the magnetic flux of the phase a must be determined first on the direction of the other phases (b y c):

$$\phi_M = \phi_{aM} cos(-120) = \phi_{aM} cos(-240) = \frac{-\phi_{aM}}{2} \tag{10}$$

$$M_s = \frac{N_{eff}\phi_M}{i_a} = \frac{N_{eff}(\frac{-\phi_{aM}}{2})}{i_a} = \frac{-L_{sM}}{2}. \tag{11}$$

For the particular case of equilibrium in the phases with the field excited by the permanent magnets and the rotor rotating at synchronous (nominal) speed, the flow trigger is given by:

$$\lambda_a = L_{ss} i_a + M_s i_b + M_s i_c = L_{ss} i_a - M_s i_a = i_a(L_{ss} - M_s) \tag{12}$$

$$\lambda_a = i_a(L_{sf} + L_{sM} + \frac{L_{sM}}{2}) = i_a(L_{sf} + \frac{3L_{sM}}{2}) = i_a L_s \tag{13}$$

where L_s is the synchronous inductance per phase. **Fig. 1** shows the equivalent circuit of a phase of the PMSG. As can be seen in comparison with the particular case of the induction generator, it can be stated that the modeling of the PMSG is much simpler and from the practical point of view it does not require additional procedures to achieve the magnetization of its coils, characteristic which makes it interesting for use in WECS applications. Particularly, this PSMG is designed with concentrated coils that produces an AC voltage with trapezoidal form which is considered a more efficient waveform to connect to power electronics. **Fig. 2** presents the trapezoidal waveform of two generated voltage phases of the six-phase PMSG.

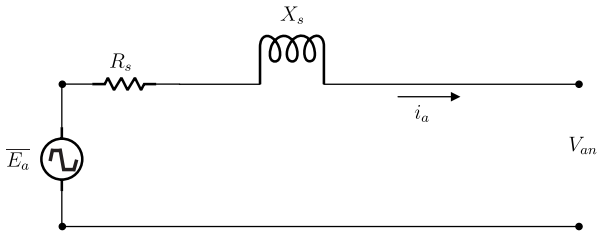

Fig. 1. Equivalent Circuit of one Phase of PMSG.

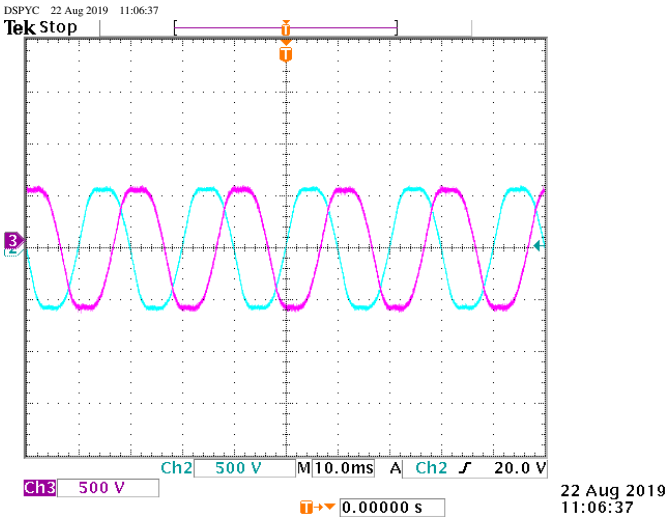

Fig. 2. Trapezoidal waveform of six-phase PMSG.

III. PROPOSED GENERATION SYSTEM SCHEME

The general scheme for the proposed grid connected AC generation system based on SpWEG and modular matrix converter (MMC) topology is shown in Fig. 3. This topology allows to inject controlled active and reactive power by means of controlling the voltage at the output capacitors v_{o1} and v_{o2} and the injected current by every module i_{g1} and i_{g2} and thus the total injected current i_g. The Phase Locked Loop (PLL) block measures the phase of the grid in order to generate a voltage synchronised with the grid voltage (v_g) at the output of every conversion stage. This process is carried out to interconnect both systems making feasible to inject power. In this way, a scheme with two control loops consisting of a combination of a predictive voltage control strategy and a current control loop that provides the voltage reference for the first one is proposed. The output capacitor of every module are connected to the point of common coupling (PCC) through a bypass switch that allows to connect the power converters to the grid once the synchronisation state is achieved.

IV. INNER PREDICTIVE VOLTAGE CONTROL LOOP

When using cascade control loops, it is important to design a fast inner-control loop to achieve a correct behaviour. Given that a known characteristic of MPC consist of fast transient response, it is particularly interesting to propose it as inner control loop strategy. MPC uses the model of the system to predict the future behaviour of it for every feasible input and chose the one that better fulfils some desired output defined by a cost function that is evaluated during every sampling time. The input that minimise the cost function is the one to be applied in the beginning of the next sampling time [25]. Before to intent to control a system based on MPC techniques, a precise model of the system is required. In this case it is needed to model first the direct matrix converter (DMC) and then the output filter. In the next section the DMC is modelled and analysed.

A. Direct Matrix Converter. Basic Principles

In this proposal, two modules of DMC are used to extract and adequate the energy from a SpWEG based on a PMSM. The scheme for every conversion module is shown in Fig. 4 where the subscript x indicates the corresponding module.

The commutation function for a simple switch is defined as:

$$S_{ij} = \begin{cases} 0, & \text{switch } S_{ij} \text{ off} \\ 1, & \text{switch } S_{ij} \text{ on} \end{cases}, \tag{14}$$

where $i \in \{u, v, w\}$ indicates the correspond input and $j \in \{a, b, c\}$ the output. Given that the input never has to be short-circuited and the current do not ever be abruptly interrupted, the follow constrains are defined:

$$S_{ui} + S_{vi} + S_{wi} = 1, \quad \forall i \in \{a, b, c\}. \tag{15}$$

Regarding about mentioned constrains, three-phase DMC is able to generates 27 valid switching states among the feasible 512 (2^9).

If the power source and load are referenced to neutral point (N_x), then it is possible to describe the relationship between the input and the output as:

$$\begin{bmatrix} v_{ax}(t) \\ v_{bx}(t) \\ v_{cx}(t) \end{bmatrix} = \begin{bmatrix} S_{ua}(t) & S_{va}(t) & S_{wa}(t) \\ S_{ub}(t) & S_{vb}(t) & S_{wb}(t) \\ S_{uc}(t) & S_{vc}(t) & S_{wc}(t) \end{bmatrix} \begin{bmatrix} v_{eux}(t) \\ v_{evx}(t) \\ v_{ewx}(t) \end{bmatrix}, \tag{16}$$

and

$$\begin{bmatrix} i_{ux}(t) \\ i_{vx}(t) \\ i_{wx}(t) \end{bmatrix} = \begin{bmatrix} S_{ua}(t) & S_{ub}(t) & S_{uc}(t) \\ S_{va}(t) & S_{vb}(t) & S_{vc}(t) \\ S_{wa}(t) & S_{wb}(t) & S_{wc}(t) \end{bmatrix} \begin{bmatrix} i_{Lxa}(t) \\ i_{Lxb}(t) \\ i_{Lxc}(t) \end{bmatrix}. \tag{17}$$

To calculate the effective voltages applied to every phase (i.e. from a, b and c to n), the common mode voltage v_{nNx} must to be subtracted from equation (16). *"Kirchoff's Current Laws"* allows to determine v_{nN} as follows:

$$v_{nNx} = \frac{v_{aNx} + v_{bNx} + v_{cNx}}{3} \tag{18}$$

Then, effective phase voltage is given by:

$$\begin{aligned} v_{anx} &= v_{aNx} - v_{nNx} \\ v_{bnx} &= v_{bNx} - v_{nNx} \\ v_{cnx} &= v_{cNx} - v_{nNx} \end{aligned} \tag{19}$$

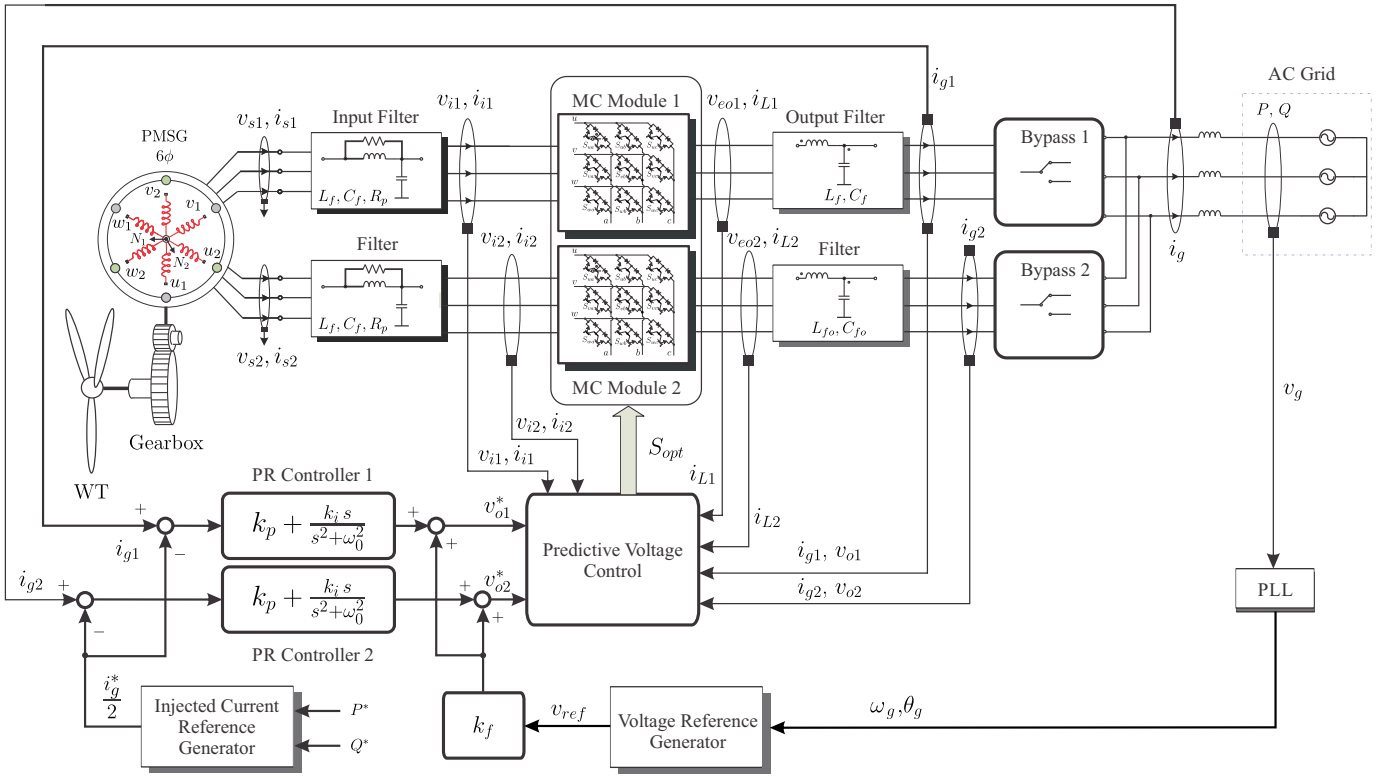

Fig. 3. Proposed multi-modular matrix converter topology applied to the SpWEG.

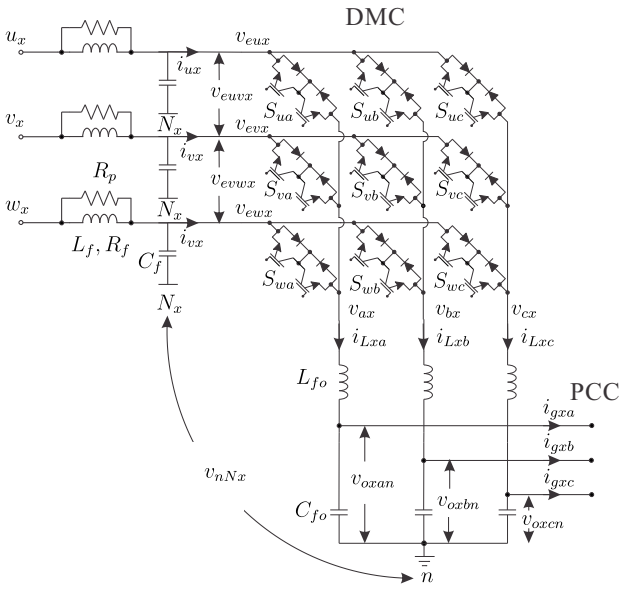

Fig. 4. Power Stage Topology.

B. Output Filter Model

Regarding the topology depicted on Fig. 4 a LC output filter is connected among the generation system and the PCC through a bypass switch. Every leg of the converter have an inductor L_{fo} with the corresponding leakage resistance R_{fo} and a capacitor C_{fo}. The inductor current i_{Lx} and the capacitor voltage v_{ox} can be taken as state variables and assuming all the parameters are the same in every leg, the system dynamic at the $\alpha-\beta$ reference plane is given by:

$$L_{fo}\frac{di_{Lx\alpha\beta}}{dt} = v_{x\alpha\beta} - v_{ox\alpha\beta} - R_{fo}i_{Lx\alpha\beta}, \tag{20}$$

where $v_{x\alpha\beta}$ corresponds the output voltage that results by applying one of the 27 valid vectors of the DMC. In the other hand, the dynamic behaviour of the voltage through the capacitor of the filter is defined as follows:

$$C_{fo}\frac{dv_{ox\alpha\beta}}{dt} = i_{Lx\alpha\beta} - i_{gx\alpha\beta}, \tag{21}$$

In this way, the system's state-space representation is given by:

$$\frac{d\mathbf{x}}{dt} = \mathbf{A}\mathbf{x} + \mathbf{B}\mathbf{u}, \tag{22}$$

where

$$\mathbf{x} = \begin{bmatrix} i_{Lx\alpha\beta} \\ v_{ox\alpha\beta} \end{bmatrix}, \quad \mathbf{A} = \begin{bmatrix} -\frac{R_{fo}}{L_{fo}} & -\frac{1}{L_{fo}} \\ \frac{1}{C_{fo}} & 0 \end{bmatrix},$$

$$\mathbf{u} = \begin{bmatrix} v_{x\alpha\beta} \\ i_{g\alpha\beta} \end{bmatrix} \text{ and } \mathbf{B} = \begin{bmatrix} \frac{1}{L_f} & 0 \\ 0 & -\frac{1}{C_f} \end{bmatrix}, \tag{23}$$

The about mentioned equations define the continuous model of the LC filter considering the output voltage of the DMC

$v_{\alpha\beta}$ and the output current injected to the grid $i_{g\alpha\beta}$ as state variables.

C. Discrete Time Model for the LC Filter

The discrete model of the system is given by:

$$\mathbf{x}(k+1) = \mathbf{A}_d\mathbf{x}(k) + \mathbf{B}_d\mathbf{u}(k), \tag{24}$$

being $\mathbf{A}_d = e^{\mathbf{A}T_s}$, $\mathbf{B}_d = \int_0^{T_s} e^{\mathbf{A}(T_s-\tau)}\mathbf{B}d\tau$, $\mathbf{A}$ and $\mathbf{B}$ are given by eq. (23) and T_s is the sampling time. Applying the about mentioned discrete model it is possible to predict the states of $v_{ox\alpha\beta}$ and $i_{Lx\alpha\beta}$ (subscript $\alpha\beta$ has been omitted in the terms of the equation) as follows:

$$i_{Lx}(k+1) = a_{11}i_{Lx}(k) + a_{12}v_{ox}(k) + b_{11}v_x(k) + b_{12}i_{gx}(k), \tag{25}$$

$$v_{ox}(k+1) = a_{21}i_{Lx}(k) + a_{22}v_{ox}(k) + b_{21}vx(k) + b_{22}i_g(k), \tag{26}$$

being

$$\mathbf{A}_d = \begin{bmatrix} a_{11} & a_{12} \\ a_{21} & a_{22} \end{bmatrix}, \mathbf{B}_d = \begin{bmatrix} b_{11} & b_{12} \\ b_{21} & b_{22} \end{bmatrix},$$

where k denotes the present sampling time and $k+1$ indicates the next. As from the preceding equations it is possible to predict the values of the current at the inductor and the output voltage in each module. Once the converter model is defined, the next step consist of design the control technique.

D. Predictive Voltage Control

The basic operating principle of the algorithm is the following: first, at the beginning of the sampling instant, new measurements of v_{ox}, i_{Lx} and i_{gx} are obtained for each module (remember that subscript x denote the corresponding module). These measurements define the starter point from which the algorithm predicts the future trajectory of the state space variables by considering equations (25) and (26), for each feasible voltage vector. Every predicted value is evaluated with a pre-designed cost function (CF), and the vector with the lowest CF is applied to the DMC switches. The presented technique is based on the proposed control in [26], [27]. In this case, the selected cost function is the following:

$$g = (v^*_{ox\alpha} - v_{ox\alpha})^2 + (v^*_{ox\beta} - v_{ox\beta})^2 + \lambda_d g_{der}, \tag{27}$$

being $v^*_{ox\alpha}$ and $v^*_{ox\beta}$ the desired voltages on the $\alpha-\beta$ plane and defining:

$$g_{der} = \left(C_{fo}\omega_{ref}v^*_{ox\beta} - i_{Lx\alpha} + i_{gx\alpha}\right)^2 + \left(C_{fo}\omega_{ref}v^*_{ox\alpha} - i_{Lx\beta} + i_{gx\beta}\right)^2. \tag{28}$$

The term g_{der} is introduced to improve the behavior saving the incapacity of the classic predictive control of tracking the capacitor voltage derivative resulting in a high total harmonic distortion (THD), creating a regulator which controls the voltage and its derivative. The effect of the derivative term is controlled with a weighting factor λ_d that was chosen considering [26]. This strategy is based on the evaluation, at every sampling instant, of the cost function g for all the valid vectors and to apply the vector which minimises the CF in the next sampling instant achieving a desired voltage tracking.

V. Outer current control loop

The proposed scheme is based on the implementation of two control loops for each converter, an internal loop corresponding to the predictive voltage control and the external loop that generates the voltage reference to inject a controlled current into the grid based on the desired power. In Fig. 3 the external control loop is shown, where the difference between the injected current per module i_{gx} and the desired current i^*_{gx} is calculated and applied as the input of a PR controller [28] which output is added to a feed-forward control signal v_{ref} which is used at system start-up to synchronise the output voltage of each conversion stage v_{ox} with the grid voltage v_g so as to be connected through a bypass. This calculated reference voltage is the input to the predictive voltage control block to calculate the optimum vector to be applied per module. The voltage v_{ref} is generated from the measurement of the phase of the grid θ_g obtained from the PLL and the amplitude of the signal of the grid. The desired current per module i^*_{gx} is a half of the necessary current i^*_g to inject the desired active and reactive power that is calculated as follows [29]:

$$i^*_{g\alpha} = \frac{2}{3}\frac{v_{g\alpha}}{v^2_{g\alpha}+v^2_{g\beta}}P^* + \frac{2}{3}\frac{v_{g\beta}}{v^2_{g\alpha}+v^2_{g\beta}}Q^* \tag{29}$$

and

$$i^*_{g\beta} = \frac{2}{3}\frac{v_{g\beta}}{v^2_{g\alpha}+v^2_{g\beta}}P^* - \frac{2}{3}\frac{v_{g\alpha}}{v^2_{g\alpha}+v^2_{g\beta}}Q^* \tag{30}$$

where P^* and Q^* denote the active and reactive power references, respectively, while $v_{gs\alpha}$ and $v_{g\beta}$ are the grid voltages in stationary reference frame ($\alpha-\beta$).

VI. Grid connection procedure

In order to perform the grid connection, the steps described below must to be followed.

1) The predictive voltage control is used to generate an output voltage (v_{ox}) synchronised with the grid voltage (v_g) in each module. This part of the procedure is shown in Fig.5.
2) Once the voltages are synchronised, the systems are connected using the bypass, setting the power references P and Q to zero, making the injected current i_{g*} to be zero.
3) Finally, the feed-forward signal can be set to zero and all the reference voltage comes from the PR controller so it is possible to select the desired active and reactive power to be injected.

Based on the above described procedure, it is possible to evaluate the proposal based on perform some simulations using MATLAB/Simulink environment.

TABLE I
IMPLEMENTED PARAMETERS ON THE SIMULATION ENVIRONMENT.

Parameter	Description		
	Symbol	Value	Unit
Grid Voltage	v_g	311	V_p
Grid frequency	f_g	50	Hz
Generator Voltage	v_s	540	V_p
Generator frequency	f_s	50	Hz
Input Filter Resistance	R_p	100	Ω
Leakage Inductor Resistance	R_f	10	mΩ
Input Filter Inductance	L_f	2.4	mH
Input Filter Capacitance	C_f	24	μF
Sampling Time	T_s	25	μs
Sampling frequency	f_s	40	kHz
Derivative weighting	λ_d	0.2	
PR proportional constant	k_p	10	
PR integral constant	k_i	1500	
Output Filter Inductance	L_{fo}	2.4	mH
Output Filter Capacitance	C_{fo}	24	μF

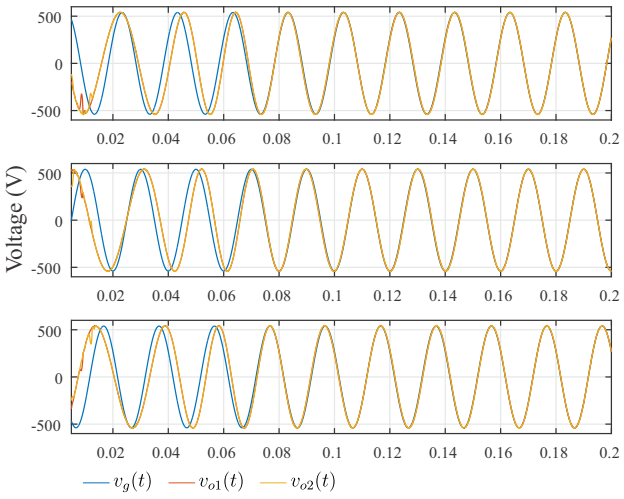

Fig. 5. Output voltage of conversion system during synchronisation process.

VII. SIMULATION RESULTS AND ANALISYS

In order to analyse and validate the proposed scheme, a simulation using the parameters depicted on Table I is performed. As was mentioned, Fig. 5 shows the synchronisation process, where it is possible to appreciate that it takes around 0.18 s to synchronise the output voltage of each module v_{o1} and v_{o2} with the grid voltage v_g. Once the synchronisation is achieved, all the subsystems are connected to the grid, holding the desired power reference to zero to avoid undesired overpeaks.

The power tracking performance and the transient response are shown in Fig. 6. Here it is possible to verify the correct tracking of active power by the response to several steps beginning with a reference of 2 kW and increasing the power in steps of 1 kW, with the reactive power set to zero. The transient response is about 2 ms that is quick enough considering the application. Related to power injection, Fig. 7 shows the phase currents response for a power reference step. Table II depicts the THD of the injected current where the desired active power

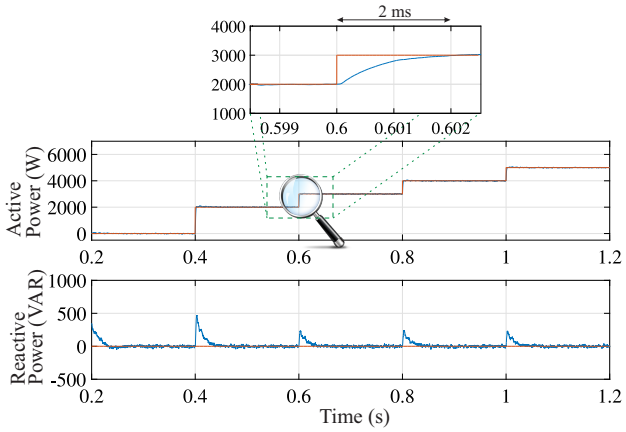

Fig. 6. Active and reactive output power supplied to the power grid.

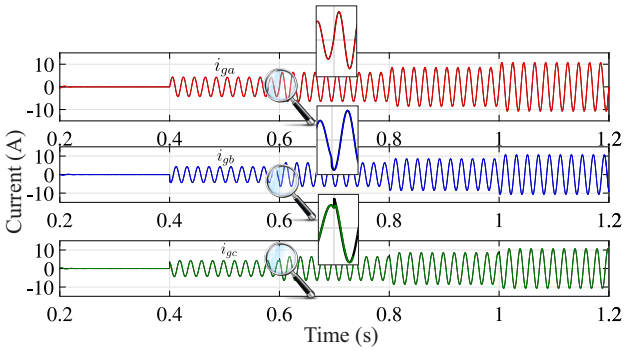

Fig. 7. Phase currents tracking of the power grid.

TABLE II
THD ANALYSIS OF THE OUTPUT CURRENT AT THE FUNDAMENTAL FREQUENCY 50 HZ.

Power	THD [%]		
	Phase a	Phase b	Phase c
2 kW	1.32	1.08	1.52
3 kW	0.62	0.57	0.67
4 kW	0.47	0.42	0.49
5 kW	0.38	0.34	0.43

was set from 2 kW to 5 kW with resulting currents of about 5 and 10 A. It can be noticed that for this values the THD plenty fulfils with the required values for grid connected systems.

VIII. CONCLUSION

After performing the about mentioned simulations, it is possible to conclude that the proposal have a correct behaviour in terms of injected power tracking with acceptable transient response and good THD regarding the international standards for DGS. The fast response of the predictive control makes feasible the implementation of a control technique that involves two cascade control loops, one internal based on Predictive Voltage control and an outer classic PR current control for indirect active and reactive power control. The

proposed topology reduce the THD using a weighted derivative tracking term in the cost function of the predictive controller allowing to improve harmonic response in contravention of worsening the reference tracking. This derivative term makes possible to implement a 1-horizon of prediction technique instead a 2-horizon one for second order systems with good response. Finally, it is possible to affirm that the proposed SpWEG based on PMSG and Multi-modular matrix converter power scheme is viable for its implementation on DGS systems controlling the injected active and reactive power with good signals quality, both in terms of transient response and harmonic content.

ACKNOWLEDGMENT

The authors express their gratitude to Consejo Nacional de Ciencia y Tecnologa de Paraguay (CONACYT), for the support and financing through Project PINV15-0584, to CONICYT of Chile through the FONDECYT Regular Project 1160690, Project MEC 80150056 and the grant CONICYT-PFCHA/Doctorado Nacional/2019-21192003.

REFERENCES

[1] V. Smil, "Distributed generation and megacities: Are renewables the answer?" *IEEE Power and Energy Magazine*, vol. 17, no. 2, pp. 37–41, March 2019.

[2] F. Blaabjerg and K. Ma, "Wind energy systems," *Proceedings of the IEEE*, vol. PP, no. 99, pp. 1–16, 2017.

[3] V. Yaramasu, B. Wu, P. C. Sen, S. Kouro, and M. Narimani, "High-power wind energy conversion systems: State-of-the-art and emerging technologies," *Proceedings of the IEEE*, vol. 103, no. 5, pp. 740–788, May 2015.

[4] S. Toledo, M. Rivera, and J. L. Elizondo, "Overview of wind energy conversion systems development, technologies and power electronics research trends," in *2016 IEEE International Conference on Automatica (ICA-ACCA)*, Oct 2016, pp. 1–6.

[5] M. J. Duran and F. Barrero, "Recent advances in the design, modeling, and control of multiphase machines: Part II," *IEEE Trans. Ind. Electron.*, vol. 63, no. 1, pp. 459–468, 2016.

[6] S. Muller, M. Deicke, and R. W. De Doncker, "Doubly fed induction generator systems for wind turbines," *IEEE Ind. Applications Magazine*, vol. 8, no. 3, pp. 26–33, 2002.

[7] O. Gonzalez, M. Ayala, J. Doval-Gandoy, J. Rodas, R. Gregor, and M. Rivera, "Predictive-fixed switching current control strategy applied to six-phase induction machine," *Energies*, vol. 12, no. 12, p. 2294, 2019.

[8] E. Levi, R. Bojoi, F. Profumo, H. Toliyat, and S. Williamson, "Multi-phase induction motor drives–a technology status review," *IET Electric Power Applications*, vol. 1, no. 4, pp. 489–516, 2007.

[9] F. Barrero and M. J. Duran, "Recent advances in the design, modeling, and control of multiphase machines: Part I," *IEEE Trans. Ind. Electron.*, vol. 63, no. 1, pp. 449–458, 2016.

[10] K. Chinmaya and G. K. Singh, "Performance evaluation of multiphase induction generator in stand-alone and grid-connected wind energy conversion system," *IET Renewable Power Generation*, vol. 12, no. 7, pp. 823–831, 2018.

[11] M. Ayala, O. Gonzalez, J. Rodas, R. Gregor, S. Toledo, J. Doval-Gandoy, and M. Rivera, "Modeling and analysis of dual three-phase self-excited induction generator for wind energy conversion systems," in *2017 IEEE Southern Power Electronics Conference (SPEC)*. IEEE, 2017, pp. 1–6.

[12] H. Fang, Z. Zhang, X. Feng, and R. Kennel, "Ripple-reduced model predictive direct power control for active front-end power converters with extended switching vectors and time-optimised control," *IET Power Electronics*, vol. 9, no. 9, pp. 1914–1923, 2016.

[13] F. M. Serra and C. H. De Angelo, "IDA-PBC controller design for grid connected front end converters under non-ideal grid conditions," *Electric Power Systems Research*, vol. 142, pp. 12–19, 2017.

[14] C. D. Fuentes, C. A. Rojas, H. Renaudineau, S. Kouro, M. A. Perez, and T. Meynard, "Experimental validation of a single DC bus cascaded H-bridge multilevel inverter for multistring photovoltaic systems," *IEEE Trans. Ind. Electron.*, vol. 64, no. 2, pp. 930–934, 2016.

[15] Y. Yu, G. Konstantinou, C. D. Townsend, R. P. Aguilera, and V. G. Agelidis, "Delta-connected cascaded H-bridge multilevel converters for large-scale photovoltaic grid integration," *IEEE Trans. Ind. Electron.*, vol. 64, no. 11, pp. 8877–8886, 2016.

[16] H. D. Tafti, A. I. Maswood, G. Konstantinou, J. Pou, K. Kandasamy, Z. Lim, and G. H. Ooi, "Low-voltage ride-thorough capability of photovoltaic grid-connected neutral-point-clamped inverters with active/reactive power injection," *IET Renewable Power Generation*, vol. 11, no. 8, pp. 1182–1190, 2016.

[17] F. Faraji, A. Hajirayat, A. A. M. Birjandi, K. Al-Haddad *et al.*, "Single-stage single-phase three-level neutral-point-clamped transformerless grid-connected photovoltaic inverters: Topology review," *Renewable and Sustainable Energy Reviews*, vol. 80, pp. 197–214, 2017.

[18] T. Dragicevic, C. Zheng, J. Rodriguez, and F. Blaabjerg, "Robust quasi-predictive control of lcl-filtered grid converters," *IEEE Trans. Power Electron.*, 2019.

[19] F. Gavilan, D. Caballero, S. Toledo, E. Maqueda, R. Gregor, J. Rodas, M. Rivera, and I. Araujo-Vargas, "Predictive power control strategy for a grid-connected 2L-VSI with fixed switching frequency," in *2016 IEEE International Autumn Meeting on Power, Electronics and Computing (ROPEC)*. IEEE, 2016, pp. 1–6.

[20] D. Pérez-Estévez, J. Doval-Gandoy, A. G. Yepes, O. Lopez, and F. Baneira, "Enhanced resonant current controller for grid-connected converters with LCL filter," *IEEE Transactions on Power Electronics*, vol. 33, no. 5, pp. 3765–3778, 2017.

[21] D. Pérez-Estévez, J. Doval-Gandoy, A. G. Yepes, Ó. López, and F. Baneira, "Generalized multifrequency current controller for grid-connected converters with LCL filter," *IEEE Transa. Ind. Appl.*, vol. 54, no. 5, pp. 4537–4553, 2018.

[22] S. Toledo, M. Rivera, R. Gregor, J. Rodas, and L. Comparatore, "Predictive current control with reactive power minimization in six-phase wind energy generator using multi-modular direct matrix converter," in *2016 IEEE ANDESCON*, Oct 2016, pp. 1–4.

[23] S. Toledo, R. Gregor, M. Rivera, J. Rodas, D. Gregor, D. Caballero, F. Gaviln, and E. Maqueda, "Multi-modular matrix converter topology applied to distributed generation systems," in *8th IET International Conference on Power Electronics, Machines and Drives (PEMD 2016)*, April 2016, pp. 1–6.

[24] G. P. R. Reddy, J. C. Sekhar, B. Naresh, and M. V. Kumar, "Comparative analysis of flying capacitor and H-bridge multilevel matrix converters for DFIG based wind energy conversion system," in *Emerging Trends in Electrical, Communications, and Information Technologies*. Springer, 2020, pp. 309–320.

[25] T. Geyer, *Model Predictive Control of High Power Converters and Industrial Drives*. Wiley, 2016. [Online]. Available: https://books.google.com.py/books?id=ovVmCgAAQBAJ

[26] T. Dragičević, "Model predictive control of power converters for robust and fast operation of ac microgrids," *IEEE Transactions on Power Electronics*, vol. 33, no. 7, pp. 6304–6317, 2018.

[27] T. Dragicevic, C. Zheng, J. Rodriguez, and F. Blaabjerg, "Robust quasi-predictive control of lcl-filtered grid converters," *IEEE Trans. Power Electron.*, pp. 1–1, 2019.

[28] S. A. Richter and R. W. De Doncker, "Digital proportional-resonant (pr) control with anti-windup applied to a voltage-source inverter," in *Proceedings of the 2011 14th European Conference on Power Electronics and Applications*, Aug 2011, pp. 1–10.

[29] Y. Bak, E. Lee, and K.-B. Lee, "Indirect matrix converter for hybrid electric vehicle application with three-phase and single-phase outputs," *Energies*, vol. 8, no. 5, pp. 3849–3866, 2015.